Experimental Gerontology 175 (2023) 112158

Contents lists available at ScienceDirect

Experimental Gerontology

journal homepage: www.elsevier.com/locate/expgero

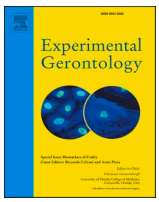

Review

Redox stress shortens lifespan through suppression of respiratory complex I in flies with mitonuclear incompatibilities

M. Florencia Camus, Enrique Rodriguez, Vassilios Kotiadis, Hugh Carter, Nick Lane *

Research Department of Genetics, Evolution and Environment, University College London, Gower Street, London WC1E 6BT, United Kingdom

A B S T R A C T

Incompatibilities between mitochondrial and nuclear genes can perturb respiration, biosynthesis, signaling and gene expression. Here we investigate whether mild mitonuclear incompatibilities alter the physiological response to redox stress induced by *N*-acetyl cysteine (NAC). We studied three *Drosophila melanogaster* lines with mitochondrial genomes that were either coevolved (WT) or mildly mismatched (BAR, COX) to an isogenic nuclear background. Responses to NAC varied substantially with mitonuclear genotype, sex, tissue and dose. NAC caused infertility and high mortality in some groups, but not others. Using tissue-specific high-resolution fluorespirometry, we show that NAC did not alter H_2O_2 flux but suppressed complex I-linked respiration in female flies, while maintaining a reduced glutathione pool. The high mortality in BAR females was associated with severe (>50 %) suppression of complex I-linked respiration, rising H_2O_2 flux in the ovaries, and significant oxidation of the glutathione pool. Our results suggest that redox stress is attenuated by the suppression of complex-I linked respiration, to the point of death in some mitonuclear lines. We propose that suppression of complex I-linked respiration is a general mechanism to maintain redox homeostasis in tissues, which could offset oxidative stress in ageing, producing a metabolic phenotype linked with epigenetic changes and age-related decline.

1. Introduction

Mitochondria are the hub of both energy transduction and intermediary metabolism. Perturbations in cell respiration can affect ATP synthesis, redox balance and Krebs cycle flux, with downstream implications for biosynthesis (Vander Heiden et al., 2009), repair (Zhong and Mostoslavsky, 2011), signaling (Martinez-Reyes and Chandel, 2020), gene expression and phenotype (Salminen et al., 2014; Wallace and Fan, 2010; Wolff et al., 2014). Despite this central position in metabolism, mitochondria are uniquely vulnerable to perturbation, as the respiratory complexes are mosaic assemblies encoded by two genomes, the mitochondrial and nuclear, which have very different rates and modes of evolution (Neiman and Taylor, 2009; Song et al., 2005). As a result, sexual reproduction generates new mitonuclear combinations in every individual, with the potential to affect all aspects of growth and development, including ageing and lifespan (Camus et al., 2012; Camus et al., 2015). Serious incompatibilities between mitochondrial and nuclear genes have been generated by introgression between divergent natural populations in a number of species (Baris et al., 2017; Barreto et al., 2018; Healy and Burton, 2020; Rank et al., 2020; Zaidi and Makova, 2019). These studies highlight the potential severity of mitonuclear incompatibilities between polymorphisms in normal populations, rather than pathological mutations known to cause mitochondrial diseases (Innocenti et al., 2011; Morrow and Camus, 2017). More subtle mitonuclear mismatches, stemming from single nucleotide polymorphisms (SNPs) can also affect gene expression and fitness (Camus et al., 2015; Mossman et al., 2017; Mossman et al., 2016), but are more likely to remain latent under benign laboratory conditions (Camus et al., 2020). If so, then the effects of subtle mitonuclear interactions might be amplified by stress, potentially unmasking hidden differences in development, health, or rates of ageing.

To gain an insight into this question, we asked whether mild mitonuclear incompatibilities alter the physiological responses to redox stress in *Drosophila melanogaster*, a model that enables tight control over mitonuclear parameters (Rand et al., 2001). *D. melanogaster* has a mitonuclear system that is closely analogous to that of humans: mtDNA encodes the same core subunits of respiratory complexes, while the global divergence between populations, in terms of mitochondrial SNPs, is also similar (Morrow et al., 2015). In this study, we therefore compared three different fly lines with subtle differences in the mitochondrial genome, all set against an isogenic nuclear background: WT (w^{1118}); COX, whose mtDNA only differs from WT by one SNP in the gene for COXII (complex IV); and BAR, which has nine SNPs difference in protein-coding mtDNA, mostly in complex I and complex IV (Fig. 1). As the three fly lines differ only in their mtDNA, the primary deficit must be in respiratory function or reactive oxygen species (ROS) flux (Blier et al., 2001; Latorre-Pellicer et al., 2016). We therefore considered how the three mitonuclear genotypes altered metabolic and phenotypic

* Corresponding author.
E-mail address: nick.lane@ucl.ac.uk (N. Lane).

https://doi.org/10.1016/j.exger.2023.112158
Received 6 February 2023; Received in revised form 17 March 2023; Accepted 22 March 2023
Available online 28 March 2023

responses to the glutathione agonist *N*-acetyl cysteine (NAC), which could potentially interfere with ROS flux, signaling and redox balance. Insofar as mitochondrial ROS signaling modulates mitochondrial biogenesis (Lane, 2011; Lane, 2012), and thus respiratory function, we anticipated that NAC might also modulate the respiratory rate. We considered low-dose (1 mg/mL) and high-dose (10 mg/mL) NAC, in line with earlier work in flies, which showed an increase in lifespan in males on 10 mg/mL NAC, but some toxicity at higher doses (Brack et al., 1997). The effect of NAC on the lifespan of female flies is more equivocal, with small benefits at lower doses (1 mg/mL) but toxicity at higher doses (Niraula and Kim, 2019; Shaposhnikov et al., 2018), which we corroborate.

We show that there are striking differences in fertility and survival between mitonuclear genotypes in males and females depending on NAC dose. We used tissue-specific high-resolution fluorespirometry to measure multiple respiratory parameters linked in real-time with H_2O_2 flux as an indication of overall ROS flux. Importantly, we found virtually no change in ROS flux in the thorax in state 3 or maximal coupled respiration under any conditions. This was not through lack of sensitivity of the method, using permeabilized tissue, as the addition of rotenone and antimycin A increased ROS flux as anticipated. Likewise, glutathione redox state generally remained stable, also indicating that the flies were not overtly redox stressed. This stable redox balance appeared to have been achieved by suppression of complex I-linked respiration, especially in female flies. While maximal respiration changed little, several measures of complex I-linked respiration were substantially lower in female flies, and especially in BAR females, where severe suppression of complex I was associated with high mortality. Rising ROS flux in the ovaries and oxidation of the glutathione pool in these flies all suggested terminal loss of redox control. Our study demonstrates that mitonuclear interactions can indeed determine individual response to redox stress, with very different outcomes in male versus female flies. We propose that suppression of complex I-linked respiration is a general mechanism to maintain redox homeostasis in tissues. This homeostatic mechanism might also apply to ageing, where increases in ROS flux and oxidative stress with age could be offset by suppression of complex I-linked respiration, resulting in a metabolic phenotype in which low complex I activity undermines ATP synthesis, metabolic flux and epigenetic state.

2. Results

2.1. Mitonuclear genotype and sex can produce extreme fitness effects in response to NAC

Both BAR and COX flies have been reported to exhibit mild male subfertility at 25 °C, which in the case of COX is exacerbated by higher temperatures (29 °C) (Camus and Dowling, 2018; Patel et al., 2016). We confirmed this effect here: both male genotypes showed a slight decrease in the noncompetitive fertility of young adults (day 12) at 25 °C (Fig. 2A). We found a significant interaction between mitochondrial genotype and NAC treatment for each sex (female: $F = 31.205$, $p \leq 0.01$; male: $F = 18.193$, $p < 0.001$). Low-dose NAC (1 mg/mL: NAC 1) had little or no effect on either male or female fertility, but high-dose NAC (10 mg/mL: NAC 10) had a severe effect on the fertility of females in all three fly lines, lowering the number of offspring by 60 to 90 %. In contrast, while NAC 10 lowered male fertility in WT and COX flies, it had no overall effect on the fertility of BAR males.

During the setup of the fitness experiment, we recorded how many flies survived NAC exposure, that is, how many flies died before measuring their fitness (Fig. 2B). Whereas NAC 1 had little effect on the survival of either male or female flies in any of the mitonuclear lines, NAC 10 clearly affected the survival of female flies (NAC: $\chi^2 = 118.862$, $p < 0.001$). In particular, BAR females were decimated by NAC 10, with barely 1 in 10 surviving to day 12 (female - mito × NAC: $\chi^2 = 13.442$, $p = 0.009$, Fig. 2B). In contrast, while NAC 10 did depress overall male survival (NAC: $\chi^2 = 20.7268$, $p < 0.001$), BAR males were unaffected. Thus, the effects of NAC 10 on survival at day 12 were sexually antagonistic in BAR flies: females mostly died, while males were barely affected by NAC 10. This pattern of sexual antagonism was not apparent in either WT or COX flies, which have fewer SNPs difference in mtDNA.

The differential fitness effects of high-dose NAC were also clear at the level of sexual organs. NAC 10 shrank the ovaries of all three fly lines (representative examples shown in Fig. 2C), matched by a collapse in embryo number (NAC: $F = 215.8642$, $p < 0.001$, Fig. 2D). Males showed

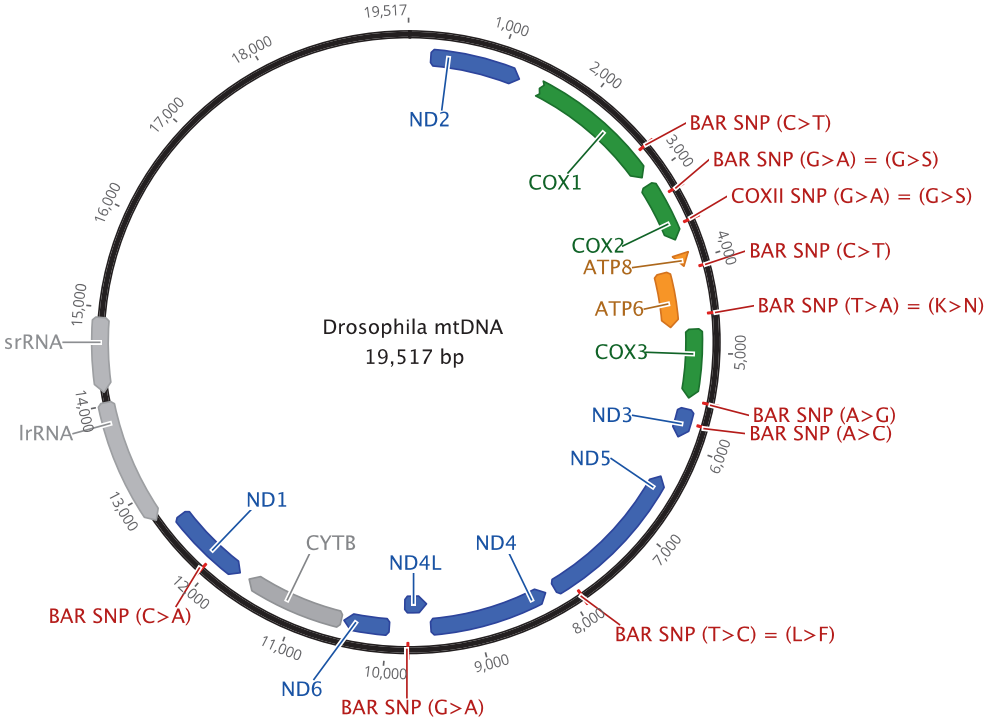

Fig. 1. mtDNA genome showing single nucleotide polymorphism (SNP) differences between mitochondrial genotypes.

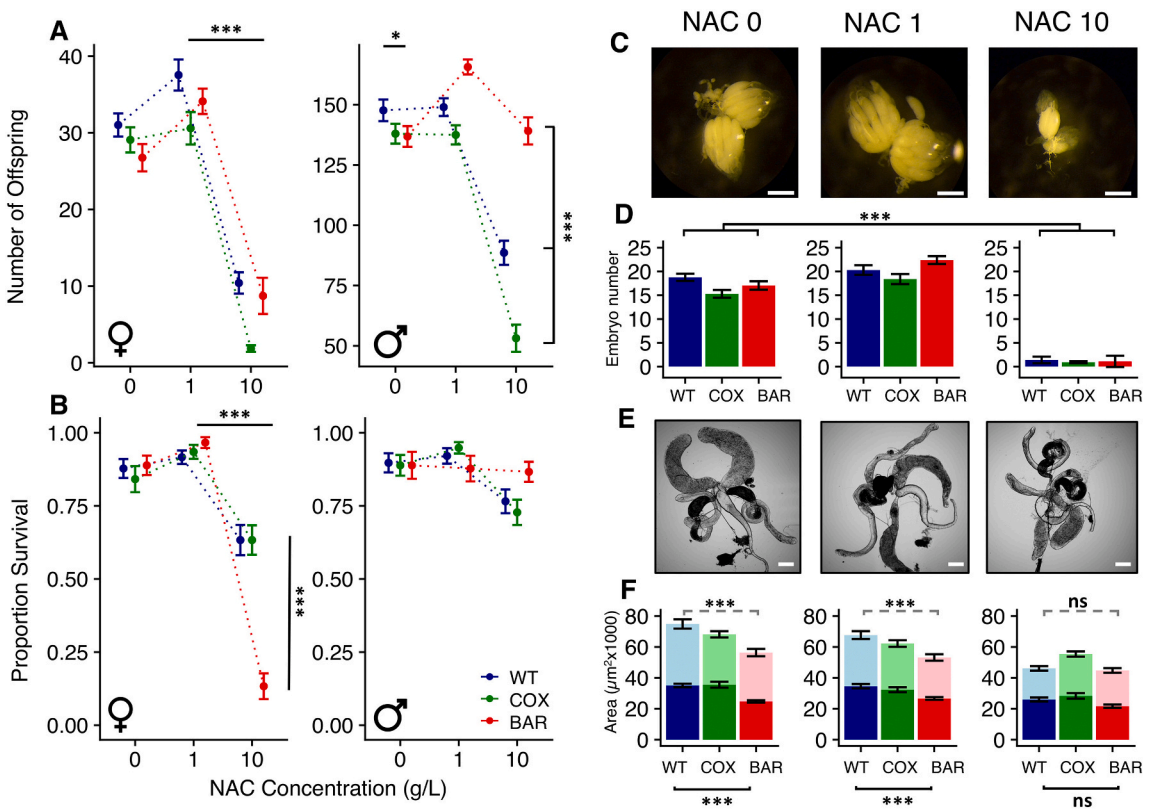

Fig. 2. Components of fitness for all mitochondrial genotypes and NAC treatments.
(A) Total number of offspring produced (mean ± SE) for males and females after a single mating event across all mitochondrial genotypes and NAC treatments. (B) Proportion of adult flies exposed to the three NAC treatments that survived to the fitness assay (day 12). (C) Images of WT ovaries after 12 days of being exposed to the three NAC treatments (representative of all 3 genotypes). (D) Quantification (mean ± SE) of ovariole number across all mitochondrial genotypes and NAC treatments. (E) Images of WT male reproductive tissue (testes, accessory glands, seminal vesicle) after 12 days exposure to the three NAC treatments. (F) Male reproductive tissue surface area (μm$^{2\times}$ 1000) for all mitochondrial genotypes across all NAC treatments (mean ± SE). Dark bars are testes surface area, whereas light bars are accessory gland measurements. Statistical significance: * $p < 0.05$; ** $p < 0.01$; *** $p < 0.001$.

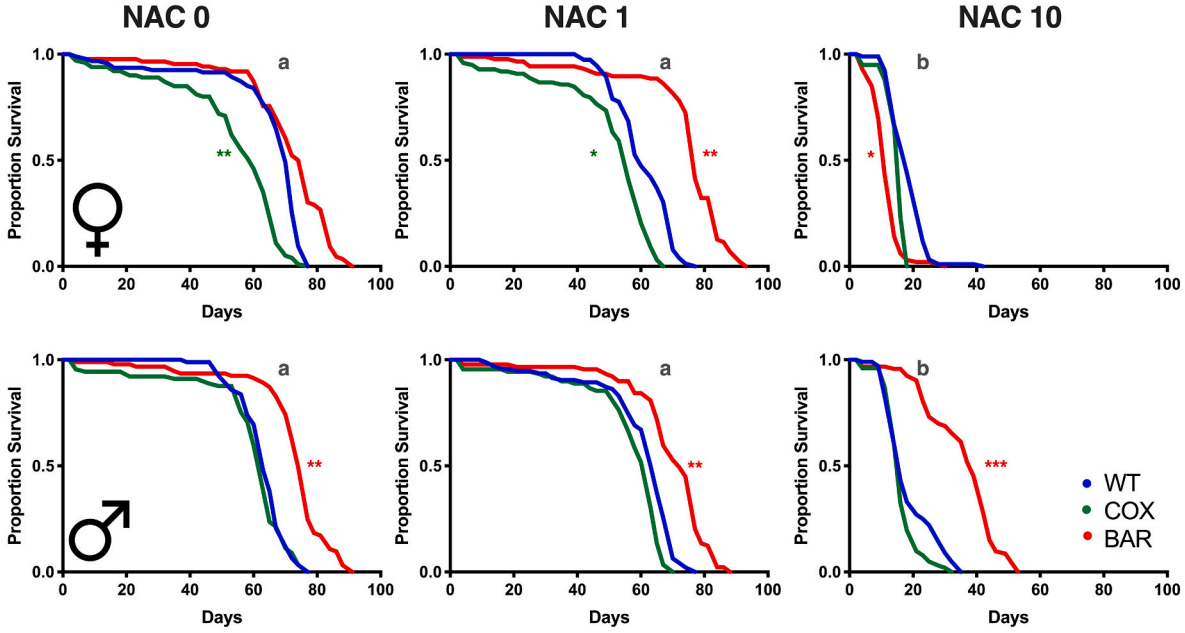

Fig. 3. Survival plots for all mitochondrial genotypes and NAC treatments.
Statistical significance: * $p < 0.05$; ** $p < 0.01$; *** $p < 0.001$ between lines receiving the same treatment; a and b signify significant differences ($p < 0.001$) between treatments across all three lines.

a more nuanced pattern (Fig. 2E and F). Untreated BAR males had smaller testes (WT_0-BAR_0: $p < 0.001$, COX_0-BAR_0: $p < 0.001$) and accessory glands (WT_0-BAR_0: $p = 0.0298$) than WT at day 12 (Fig. 2F), which corresponded to their subfertility (Fig. 2A), indicating a specific mitonuclear incompatibility in the testes. Treatment with NAC 10 shrank the testes and accessory glands of both WT and COX flies but had little further effect on BAR males (Testes-NAC: $F = 17.9905$, $p < 0.001$; Acc-NAC: $F = 17.6898$, $p < 0.001$, Fig. 2F), consistent with their uncompromised fertility at day 12 on NAC 10 (Fig. 2B).

2.2. Differences in longevity can be sexually antagonistic

Our analysis of these components of fitness indicated that fly lines with isogenic nuclear background but distinct mtDNA were affected differently by NAC at day 12. We asked whether these differences in fitness persisted across the life course. Without treatment, BAR females lived significantly longer than either WT or COX females (WT-BAR: $\chi^2 = 89.491$, $p < 0.001$; COX-BAR: $\chi^2 = 89.912$, $p < 0.001$, Fig. 3). NAC 1 had small effects on longevity, depending on the mitochondrial genotype. The lifespan of WT females was unchanged on NAC 1, while COX flies had a shorter lifespan (COX_0-COX_1: $\chi^2 = 42.144$, $p < 0.001$) and BAR females had a slight increase (BAR_0-BAR_1: $\chi^2 = 6.076$, $p = 0.009$). NAC 10 was again severely toxic to BAR females (BAR_0-BAR_{10}: $\chi^2 = 203.099$, $p < 0.001$), which were nearly all dead before day 20. However, WT and COX females were also seriously affected just a few days later (WT_0-WT_{10}: $\chi^2 = 213.729$, $p < 0.001$; COX_0-COX_{10}: $\chi^2 = 167.755$, $p < 0.001$, Fig. 3). Thus, while BAR flies were significantly worse hit by NAC, the severe toxicity of NAC 10 was not specific to BAR females (mito × NAC: $\chi^2 = 172.9350$, $p < 0.001$).

Males showed significant effects of both mitochondrial genotype and NAC on longevity (mito × NAC: $\chi^2 = 172.9350$, $p < 0.001$, Fig. 3). Without treatment, COX flies were significantly shorter lived than either WT or BAR males ($p < 0.05$). NAC 1 abolished the difference between WT and COX flies, with both groups now displaying similar longevity (Fig. 3). In contrast, BAR males had significantly longer lifespan than either of those groups ($p < 0.05$). As in females, NAC 10 again had severe toxicity in all groups, albeit less devastating for males (Fig. 3). In this case, far from being the worst hit, BAR males had relatively long lifespan (WT_{10}-BAR_{10}: $\chi^2 = 67.398$, $p < 0.001$; COX_{10}-BAR_{10}: $\chi^2 = 159.288$, $p < 0.001$), again exhibiting signatures of sexual antagonism.

2.3. Metabolic profile and effect of NAC vary by tissue

We employed tissue-specific high-resolution fluorespirometry to simultaneously measure respiratory rates and H_2O_2 flux for two tissues (thorax and reproductive) in each sex. We chose to first inspect for broad patterns using Principal Components Analysis (PCA), with results showing distinct metabolic profiles for different tissue (Fig. 4; for loadings see Fig. S1 and Table S1). Male and female thoraces exhibited overlapping metabolic profiles, whereas reproductive organs diverged from the thoraces. From the PCA loadings we know that much of the variance captured by PC1 is related to oxygen metabolism, whereas variance for PC2 is driven by H_2O_2 flux. Based on this, we can infer that ovaries had much lower metabolic rates and lower stress, while testes had similar metabolic profile to ovaries, but significantly more stress. While it is possible that we over-estimated metabolic stress by homogenizing the testes and accessory organs compared with permeabilizing muscle fibers, we homogenised ovaries using the same methodology, yet H_2O_2 flux was >10-fold greater relative to oxygen consumption in the testes compared with the ovaries (i.e. ROS flux ratio, Fig. S2). Clearly NAC 10 significantly affected the ovaries, showing a major increase in stress, possibly indicating a pro-oxidant effect through reductive stress. Other shifts with NAC did not achieve statistical significance in the pooled data, but oxygen metabolism was suppressed in female versus male thoraces; in fact, the PCA plots masked specific differences in oxygen metabolism between mitonuclear lines.

2.4. NAC suppresses complex I-linked respiration, especially in vulnerable female lines

We next examined specific metabolic states across all samples (sex/nac/genotype combinations). State 3 respiration (Fig. 5) is initiated when ADP is added to pyruvate, malate and proline, and so gives an indication of respiration linked with substrates that feed electrons into the respiratory chain mainly through complex I. Because complex I-linked respiration maximizes proton pumping and so ATP yield, complex I-linked substrates tend to be utilized most when aerobic demands are high (as in the thorax here). Full traces for all respiratory states are shown in Fig. S3. We found that state 3 respiration is around one third higher in females than in males ($F = 26.6778$, $p < 0.001$, Fig. 5A and B), corroborating earlier work (Aw et al., 2017; Wolff et al., 2016b). While NAC 1 had little effect on respiratory rates, NAC 10 decreased state 3 respiratory flux in pooled female lines ($F = 4.7432$, $p = 0.011$; Fig. S4). The suppression of state 3 flux varied significantly with mitonuclear genotype ($F = 3.2287$, $p = 0.04423$). Untreated COX and BAR females had slightly lower state 3 respiration than WT, albeit still substantially higher than any of the male fly lines. While respiration was lowered across all female thoraces with NAC 10, it was severely depressed in BAR

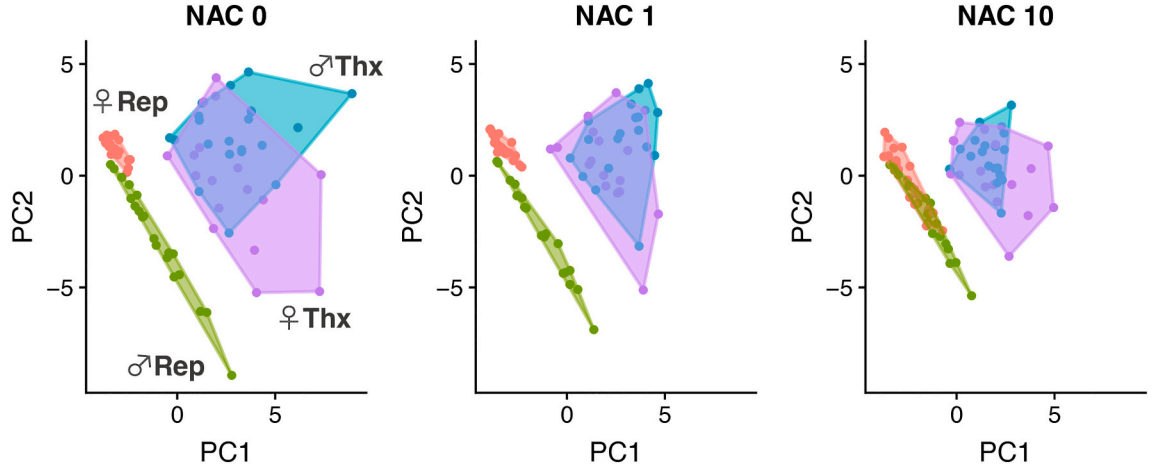

Fig. 4. Principal component analysis by tissue and NAC treatment.
Tissue-specific respirometry results for all mitochondrial genotypes combined. Respirometry data was partitioned using principal components analysis across all NAC treatments. The first two principal components account for most of the variance (PC1 = 54.03 % and PC2 = 36.52 %). For loadings see Fig. S1.

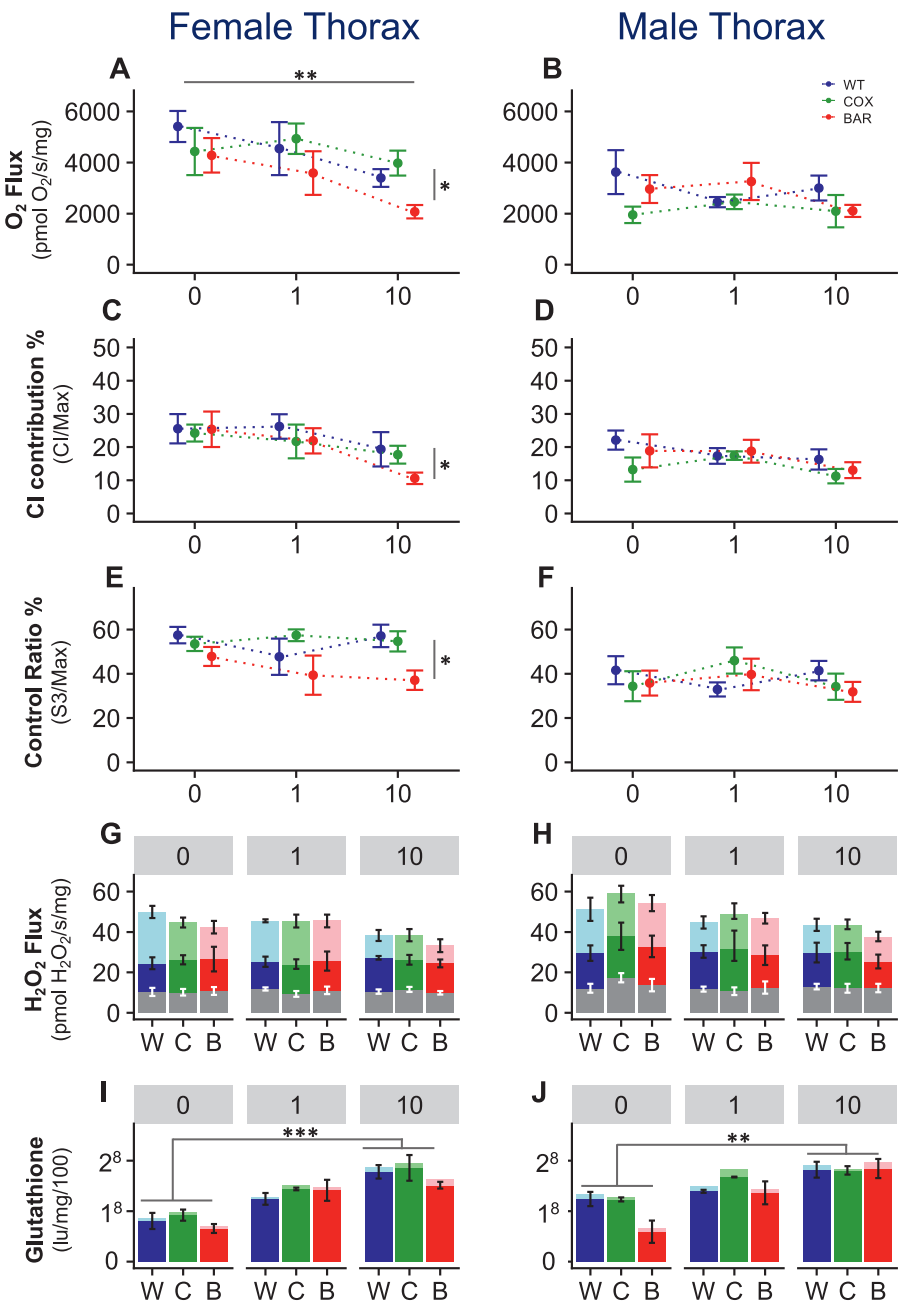

Fig. 5. Oxygen flux, H_2O_2 flux and redox balance in thoraces

Fluorespirometry and glutathione results (mean ± SE) for female (left) and male (right) thoraces for all mitochondrial genotypes and NAC treatments. (A and B) State 3 O_2 flux; (C and D) complex I contribution; (E and F) control ratio; (G and H) H_2O_2 flux; (I and J) glutathione concentration. For H_2O_2 flux, grey bars denote state 3 flux; dark-coloured bars denote flux after addition of rotenone; and light-coloured bars show flux after addition of antimycin A. For glutathione samples, dark-coloured bars show reduced glutathione and light-coloured bars oxidized glutathione, with the combined coloured area being total GSH. Statistical significance: * $p < 0.05$; ** $p < 0.01$; *** $p < 0.001$.

females (WT-BAR: $p = 0.0402$, COX-BAR: $p = 0.0046$, Fig. 5A and B) at day 12 – the same group whose survival was most dramatically cut by NAC 10 treatment.

Maximum coupled respiration was also significantly depressed by NAC 10 across all female genotypes in the thorax (NAC × sex: $F = 3.3013$ $p = 0.04134$, Fig. S5), but in this case to similar absolute values across all genotypes. Because survival at day 12 was ~15 % for BAR females compared with ~60 % for WT (Fig. 2), it is unlikely that the suppression of maximum respiration was responsible for the death of BAR females. This inference is reinforced by two analyses of relative respiratory rates, both of which indicate specific suppression of complex I (Fig. 5C and D). First, complex I contribution to maximum respiration (based on rotenone inhibition) roughly halved from ~25 % for WT and BAR females when untreated (NAC 0) to ~12 % of maximal respiration for BAR females on NAC 10, compared with ~20 % for WT and COX females (Fig. 5C and D). Second, the control ratio (state 3 respiration/maximum coupled respiration) fell from around 50–60 % in all untreated female lines, to <40 % in BAR females on NAC 10, while remaining above ~55 % in WT and COX females on NAC 10 (Fig. 5E and F). These findings are all consistent with the hypothesis that NAC 10 suppressed state 3 respiration, and specifically complex I activity, in the thoraces of BAR females at day 12, while sparing WT and COX flies at this same time point. The differences between complex I activity and control ratio are most likely explained by the use of proline as one of the three substrates for state 3 respiration, as this can also feed electrons directly into complex III via proline dehydrogenase (McDonald et al., 2018).

While the thoracic state 3 respiration in males was little more than half that of females, NAC 10 suppressed pooled state 3 respiration to a much lesser extent (NAC: $F = 4.7432$, $p = 0.011$, Figs. 5 and S4). In fact, on a per mg of tissue basis, the absolute rate of state 3 respiration was similar in BAR males and females on NAC 10; the difference lay in the

degree of suppression relative to untreated controls (~20 % for males versus ~50 % for females). Despite their lower state 3 respiration, male mortality at day 12 was limited in comparison with females. In contrast, the difference in maximum respiration was less pronounced, at around 15 %, suggesting that male flies are better able to survive on complex III-linked substrates such as glycerol phosphate (Fig. S5). Furthermore, none of the male groups showed significant depression in maximum coupled respiration on NAC 10 (Fig. S5). This tendency for male flies to depend less on complex I-linked substrates (Aw et al., 2017) was confirmed by complex I activity and control ratios (Fig. 5D and F). CI activity was ~20 % lower, and control ratio ~ 30 % lower than females, but these values were not significantly depressed by NAC 10 in any fly line. Taken together, these results suggest that male flies have less need for complex I-linked respiration than females, and this lower dependence may partially protect males against NAC toxicity.

2.5. Respiratory suppression at complex I maintains redox balance in the thorax

Given the major differences in respiratory control between males and females, and between different mitonuclear lines, H_2O_2 flux remained remarkably stable in the thoraces of both male and female flies (Figs. 5G and H, and S6). Total glutathione levels increased significantly with higher doses of NAC across all tissues (NAC_0-NAC_1: $p < 0.001$, NAC_0-NAC_{10}: $p < 0.001$). This confirms that the flies did indeed ingest NAC with their food, and that it had the anticipated effect of raising tissue glutathione levels, with NAC 10 raising thoracic glutathione levels more than NAC 1 (NAC_1-NAC_{10}, $p < 0.001$, Fig. 5I and J). Despite this sustained increase in glutathione levels in both male and female thoraces, state 3 H_2O_2 flux generally remained stable, while as noted previously, respiration was suppressed, mainly at complex I, and especially in BAR females.

Despite the substantial rise in thoracic glutathione levels with NAC, the ratio of oxidized to reduced glutathione barely changed with increasing NAC dose, suggesting that modulation of ROS flux prevented the oxidation of the glutathione pool, maintaining redox homeostasis in the thorax (Fig. S7). The effect of respiratory inhibitors suggests that ROS flux was indeed modulated by suppression of respiration. The respiratory inhibitors also notably demonstrate that H_2O_2 flux did derive from the mitochondrial respiratory chain, and that our methodology was sufficiently sensitive to measure changes in H_2O_2 flux in permeabilized thoraces. The stacked bars of Fig. 5G and H show H_2O_2 flux after inhibition of maximum respiration at complex I, using rotenone, and at complex III, using antimycin A. The stacked bars reflect cumulative H_2O_2 flux, i.e. ROS flux increased on addition of rotenone and again on addition of antimycin A. These measurements demonstrate that the H_2O_2 flux derives from mitochondrial complexes I and III rather than from elsewhere in the cell. Most importantly, the total change in H_2O_2 flux was very similar in response to rotenone in the thoraces of both male and female flies of all mitonuclear lines, and with all doses of NAC. This implies that the maximum reactivity of complex I to oxygen remained stable across all these states. That this low reactivity was achieved by limiting the number of reactive ROS-generating centres in complex I was shown by the corresponding suppression of complex I activity and state 3 respiration on NAC 10. Most ROS are thought to derive from complex I under physiological conditions (Mallay et al., 2019; Murphy, 2009; Quinlan et al., 2013), hence state 3 respiration is preferentially suppressed. This interpretation is borne out by ROS flux ratios (Fig. S2), which show little to no change in maximal H_2O_2 flux per unit oxygen consumption in the maximal coupled respiratory state (max H_2O_2/max coupled respiration), reflecting the most physiological input of electrons from multiple substrates simultaneously.

2.6. NAC disrupts redox balance in sex organs

The tight control of redox balance in the thoraces of flies was lost in the sexual organs with NAC 10. In terms of overall dynamics, respiratory control in the ovaries reflected that in the thoraces, albeit at ~10-fold lower flux levels (Figs. 6 and S4). This difference may have partly reflected tissue damage from homogenization (which was, even so, the most reliable preparation method for delicate sex organs). While the different preparations meant that direct comparisons should not be made between flux rates in the thoraces and sex organs, the patterns of respiratory control were reliable, and could be compared between ovaries and testes prepared using the same methods. These again showed sexually antagonistic responses in the reproductive tissues (NAC × sex: $F = 11.7907$, $p < 0.001$, Fig. S5). In the ovaries, NAC treatment suppressed both state 3 and maximum respiration (Figs. 6; S4 and S5). Unlike the thorax, however, maximum respiration was more strongly reduced than state 3 respiration. In contrast, in male reproductive tissue, NAC 10 tended to increase both state 3 and maximum respiration (Figs. 6; S4 and S5). H_2O_2 flux was less tightly constrained in the reproductive tissue, increasing with NAC in the ovaries, and significantly so in BAR flies on NAC 10, while falling slightly in testes and accessory glands on NAC 10 (NAC × sex: $F = 6.2105$, $p = 0.002$, Fig. 6). Tissue-specific glutathione levels rose on NAC 10 in all cases, and dramatically so in BAR females, where glutathione levels rose around 8-fold compared with the other genotypes (Fig. 6). Despite these shifts, the ratio of oxidized to reduced glutathione remained stable in the ovaries, and tended to become more oxidized in the testes and accessory glands (Fig. S7). However, the suggestion that glutathione pool became more oxidized in BAR females in both thoraces and ovaries was borne out by pooling data from both organs (Fig. S8). In this case, the glutathione pool was significantly more oxidized in BAR females, indicating redox stress in this group alone – the group that were mostly dying by day 12.

The main reason why ovaries tended to lose redox balance again appears to be a dependence on complex I-linked respiration. Complex I contribution was nearly 40 % greater in the ovaries than in the thoraces (~34 % vs. ~25 %) in all three mitonuclear lines (Figs. 5C and 6C). Likewise, the control ratio was 50–60 % in the ovaries, as high as in the thoraces and about a third higher than in the testes, again implying a high demand for ATP synthesis through complex I-linked respiration, most probably reflecting the high metabolic costs of egg production (Lee et al., 2008; Trivers and Campbell, 1972) (Fig. 6E). NAC 10 strongly suppressed complex I contribution in both COX and BAR flies, to around 10 % of maximum respiration (Fig. 6C), with the control ratio falling to 40–50 % (Fig. 6E). Notably, BAR females on NAC 10 had significantly elevated H_2O_2 flux in normal state 3 respiration ($p = 0.0472$, Fig. 6G) and after rotenone inhibition ($p = 0.0326$, Fig. 6G). Presumably, suppression of complex I activity was not sufficient restrict ROS flux. This failure to retain redox balance through respiratory modulation was also indicated by a sharp rise in the ROS flux ratio (max H_2O_2/max O_2) in the ovaries in all three mitonuclear lines on NAC 10 (NAC × sex: $F = 12.3134$, $p < 0.001$, Fig. S2).

H_2O_2 flux in the male reproductive tissues is difficult to decipher, being high in almost all respiratory states, especially given the very low rates of respiration in the male sex organs – around 20-fold lower than the male thoraces. While these values might in part reflect tissue damage during homogenization, they also probably reflect specialization of mitochondria to processes other than ATP synthesis, which is known to contribute relatively little in sperm (Wetzker and Reinhardt, 2019) and stem cells (Lord and Nixon, 2020). For example, ROS may drive cell growth and proliferation through transcription factors such as $HIF_{1\alpha}$ (Hamanaka and Chandel, 2010). This interpretation is supported by the relatively low H_2O_2 flux in the reproductive tissues of untreated BAR males (NAC 0; Fig. 6H), which corresponded to significant male subfertility (Fig. 2A). NAC 1 slightly increased H_2O_2 flux in BAR males (Fig. 6H), as well as state 3 (Fig. 6B) and maximal coupled (Fig. S5) respiration, all of which were linked with significantly improved fertility (Fig. 2A). While NAC 10 reversed many of these metabolic effects in BAR males (Figs. 6 and S5) the total glutathione pool was restricted in size more successfully than in other fly lines (Fig. 6), corresponding to

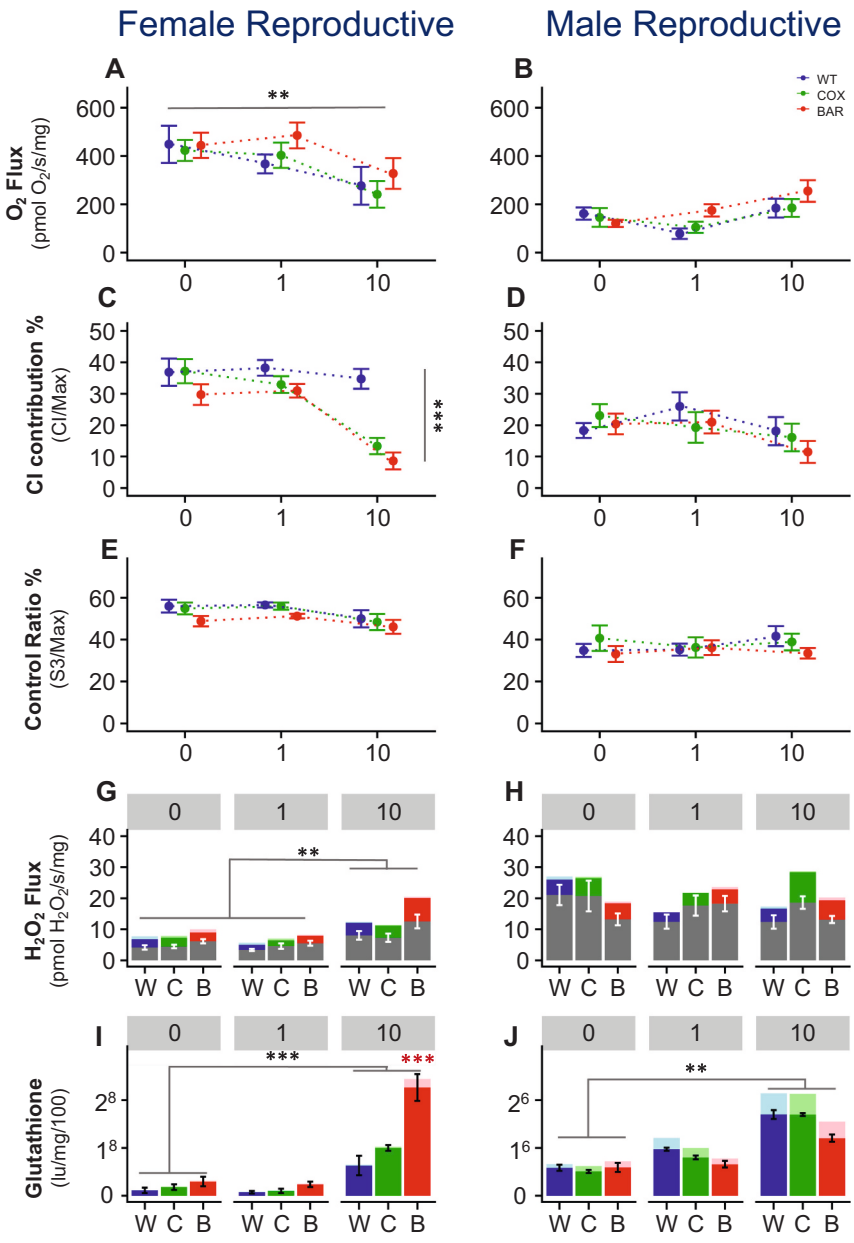

Fig. 6. Oxygen flux, H_2O_2 flux and redox balance in reproductive tissues

Fluorespirometry and glutathione results (mean ± SE) for female (left) and male (right) reproductive tissues, for all mitochondrial genotypes and NAC treatments. (A and B) State 3 O_2 flux; (C and D) complex I contribution; (E and F) control ratio; (G and H) H_2O_2 flux; (I and J) glutathione concentration. For H_2O_2 flux, grey bars denote state 3 flux; dark-coloured bars denote flux after addition of rotenone; and light-coloured bars show flux after addition of antimycin A. For glutathione samples, dark-coloured bars show reduced glutathione and light-coloured bars oxidized glutathione, with the combined coloured area being total GSH. Statistical significance: * $p < 0.05$; ** $p < 0.01$; *** $p < 0.001$.

virtually unimpaired fertility in young adults (Fig. 2B). There were no differences in the oxidation state of the glutathione pool in either the testes (Fig. S7) or whole BAR flies (Fig. S8).

3. Discussion

Differences in mitonuclear genotype are generated between individuals by sexual reproduction every generation. These differences can be amplified by stress, potentially driving disparities in phenotypic outcomes including fertility and lifespan (Montooth et al., 2019; Zhu et al., 2014). We have used a *Drosophila* model to investigate whether subtle mitonuclear interactions alter physiological responses to redox stress induced by *N*-acetyl cysteine (NAC), an antioxidant that promotes glutathione synthesis (Samuni et al., 2013) but can also cause reductive stress (Korge et al., 2015; Xiao and Loscalzo, 2020; Zhang et al., 2012) at higher concentrations. In untreated flies, mitonuclear interactions had relatively mild phenotypic effects, notably male subfertility (Fig. 2) and moderate (<20 %) differences in median lifespan (Fig. 3). These subtle mitonuclear interactions underpinned critical differences in response to high-dose NAC (10 mg/mL). NAC 10 did not alter H_2O_2 flux in the thorax but suppressed complex I-linked respiration in female flies (Fig. 5), while generally maintaining a reduced glutathione pool (Figs. 5 and S8). BAR flies, which differ from wild-type in just 9 SNPs in protein-coding mtDNA (Fig. 1) showed dramatic sexually antagonistic responses to NAC. Male flies were not affected by NAC 10 in either survival or fertility at day 12 (Fig. 2) but most females had died by then, with the few survivors also showing severely compromised fertility (Fig. 2). This high mortality rate in BAR females was associated with severe suppression of complex I-linked respiration (> 50 % suppression) in the thoraces (Fig. 5) and ovaries (Fig. 6), rising H_2O_2 flux in ovaries (Fig. 6) and oxidation of the glutathione pool in pooled tissues (Fig. S8), indicating a loss of redox control.

Our findings suggest that suppression of complex I-linked respiration might act as a general mechanism to lower redox stress in tissues, maintaining redox homeostasis. In the thorax, state-3 H_2O_2 flux is remarkably stable in males and females of all three fly lines, regardless of treatment, despite very large differences in the rate of complex I-linked respiration (Fig. 5). Our inference, that H_2O_2 flux is stabilized

within homeostatic limits by suppression of complex I, is supported by the effects of rotenone inhibition, which were also remarkably consistent in both sexes of all fly lines, and on all treatments (Fig. 5). The fact that rotenone inhibition increased H_2O_2 flux confirms that our fluororespirometry method is sensitive enough to measure changes in ROS flux in permeabilized fibers, and that the ROS flux measured does indeed derive from the respiratory chain rather than other places in the cell. H_2O_2 flux from complex I is constrained by the architecture of the system: inhibition of complex I by rotenone has to increase ROS flux in proportion to the number and reactivity of ROS-generating centers in complex I (Barja, 2013). The fact that rotenone-inhibited H_2O_2 flux was similar in all cases, even though complex I-linked respiration had been suppressed to a much greater degree in females than males, and in BAR females in particular, likely reflects a smaller number of more reactive ROS-generating centers. If so, then suppression of complex I lowered total ROS flux back to within tight homeostatic limits. Others have also reported that suppression of complex I can lower ROS flux from mitochondria (de Paula et al., 2013; Rodriguez-Nuevo et al., 2022). Long-term redox balance is governed in part by the S-glutathionylation of proteins, which can suppress complex I-linked respiration in response to oxidation of the glutathione pool (Beer et al., 2004; Mailloux, 2020; Mailloux and Willmore, 2014), though we have not established this as a specific mechanism here. Degradation of unstable oxidized complex I has also been reported (Guarás et al., 2016).

Our hypothesis is supported by the stable ROS flux ratio (H_2O_2 flux in relation to maximal coupled respiration; Fig. S4), and the reduced glutathione pool (Figs. S7 and S8), which together indicate that suppression of complex I maintains normal redox balance. Strikingly, suppression of complex I is more pronounced and costly in female flies, where the high metabolic costs of egg production (Lee et al., 2008; Trivers and Campbell, 1972) might demand greater complex I dependence in the ovaries. That is because complex I-linked respiration maximizes mitochondrial NADH oxidation, promoting both ATP synthesis and Krebs-cycle flux, which provides key precursors for biosynthesis (Inigo et al., 2021; Sweetlove et al., 2010; Vander Heiden et al., 2009; Weinberg and Chandel, 2009). Such physiological limitations on the capacity to suppress complex I may account for the rise in H_2O_2 flux in the ovaries on NAC 10 in BAR females. The inference that NAC 10 can induce reductive stress is supported by the clear oxidation of the glutathione pool in BAR females alone (Fig. S8). We infer that increased ROS flux from heavily reduced (so more reactive) respiratory complexes was compensated by down-regulation of complex I, suppressing state 3 respiration to the limits where redox control was lost, which likely caused the death of female BAR flies (Fig. 2).

While our interpretation linking respiratory suppression to redox balance has not yet been proved (ongoing transcriptomic and metabolomic work will address these questions) there is little doubt that subtle differences in mitonuclear genotype can induce extreme differences in response to redox stress through NAC supplementation. The fly model utilized here enables tight control over mitonuclear variables, which allows us to demonstrate very clear effects against an isogenic nuclear background. In terms of their nuclear genes, these mitonuclear fly lines are equivalent to identical twins, so the stark differences in physiological and phenotypic outcomes between them are revealing. While tissues such as testes can express distinct nuclear isoforms of mitochondrial genes (Eslamieh et al., 2017; Gallach et al., 2010; Havird and McConie, 2019) the isogenic nuclear background of our fly lines means that such variations cannot explain our data. In humans, most individuals will differ from each other in at least as many SNPs in mtDNA as the fly lines reported here, while also varying in their nuclear alleles, which would be expected to modulate the risk (Bénit et al., 2010; Morrow and Camus, 2017). We know from mitochondrial diseases that nuclear variations can indeed suppress or unmask severe symptoms (McFarland et al., 2002; Morrow and Camus, 2017), but the extent to which ordinary SNPs in both mitochondrial and nuclear genes influence life-long health, risk of disease, age-related decline or drug responses is simply unknown. The iceberg of missing hereditability has long confounded understanding of genetic risk factors from genome-wide association studies (Manolio et al., 2009), yet the relative risk associated with specific nuclear SNPs should vary in unpredictable ways depending on their interactions with mitochondrial SNPs, whether direct or indirect. Mitochondrial SNPs are often neglected on the grounds that there are very few of them compared with nuclear SNPs, but their importance to ATP synthesis, redox balance, biosynthesis, signaling and gene expression mean they have a greater potential to amplify risk (Pesole et al., 2012). Our results demonstrate that subtle mitonuclear interactions not normally associated with overt disease can indeed cause unexpected differences in physiological response to redox stress. Such effects are likely to be pervasive, and mitonuclear interactions should be considered as a potentially key contributors to personalized medicine.

Finally, our work suggests a novel interpretation of the possible role of ROS in ageing, which could account for a number of observations that seem to contradict the notion that ROS play a driving role in ageing (Lane, 2022). The current consensus holds that, while ROS can cause oxidative damage, they are important signaling molecules (Hamanaka and Chandel, 2010), so their role is more nuanced (Brand, 2016; Morgan et al., 2016; Sobotta et al., 2015; Willems et al., 2015); that antioxidant supplements do not extend lifespan, nor do they usually protect against age-related diseases (Bjelakovic et al., 2014; Bjelakovic et al., 2007; Halliwell, 2011; Halliwell, 2013); that the accumulation of mutations in mtDNA does not correlate with the rate of ageing (Ameur et al., 2011; Kauppila et al., 2017; Trifunovic et al., 2005); and that most new mutations in mtDNA in animals are caused by copying errors rather than oxidative damage (Lagouge and Larsson, 2013; Larsson, 2010). The results presented here suggest that any increase in oxidative stress with age would tend to be offset by a suppression of complex I-linked respiration. Because complex I is the main sink for NADH in the mitochondrial matrix, suppression of complex I affects not only ATP synthesis but also metabolic flux (Inigo et al., 2021; Sweetlove et al., 2010; Weinberg and Chandel, 2009): a shift the NAD/NADH ratio impacts on Krebs cycle flux and the provision of precursors for biosynthesis (Lane, 2022; Martinez-Reyes and Chandel, 2020; Picard and Shirihai, 2022; Vander Heiden et al., 2009). Changes in steady-state concentration of Krebs cycle intermediates can have potent epigenetic effects, as can shifts in NAD/NADH ratio, ATP/ADP ratio and acetyl CoA availability (D'Aquila et al., 2015; Kopinski et al., 2019; Wallace and Fan, 2010). All these concerted changes act downstream from the suppression of complex I, on the mTOR/sirtuin axis (Ji et al., 2022; Khan et al., 2017; Nacarelli et al., 2015; Wei et al., 2015), and likely manifest as a pseudo-program (Blagosklonny, 2013). Complex I is increasingly seen as a critical hub determining lifespan (Mota-Martorell et al., 2020; Pamplona et al., 2021), as well as susceptibility to age-related diseases ranging from Alzheimer's disease to cancer (Forte et al., 2019; Gui et al., 2016; Holper et al., 2019; Quiros et al., 2016; Rodenburg, 2016; Vasan et al., 2020). The simple conception that ROS flux is maintained within tight homeostatic limits by suppression of complex I can explain why oxidative stress with age is limited; why ROS flux is mostly stable; why antioxidants have little benefit; why de novo mtDNA mutations do not correlate with ageing; why ATP synthesis and metabolic flux shift with age to a senescent phenotype; and why epigenetic changes mimic a pseudo-program for ageing.

4. Materials and methods

4.1. *D. melanogaster* maintenance and strains

All *Drosophila melanogaster* stock strains were maintained on a standard mix of molasses/cornmeal medium at a constant 25 °C on a 12/12 light dark cycle. Three different strains of *D. melanogaster* were used in this experiment, differing only in their mitochondrial genomes. The "WT" strain is the coevolved strain, with the $w^{1118–5095}$ nuclear genome naturally coevolved with the mitochondrial genome. The second strain

has the same isogenic $w^{1118–5095}$ nuclear background but has a mitochondrial haplotype termed "COXII". The COXII haplotype is derived from $w^{1118–5095}$ flies in which the mitochondrial mutation $COII^{G177S}$ has become fixed (Patel et al., 2016). $COII^{G177S}$ is a single non-synonymous change to subunit II of cytochrome C oxidase, and this SNP is the only difference between COXII and WT mtDNA (Fig. 1). The third strain has a mitochondrial haplotype designated BAR, and is derived from a wild population from Barcelona, Spain. For this strain, the original chromosomes have been replaced by those of the $w^{1118–5095}$ nuclear genome through the use of a balancer chromosome crossing scheme (Clancy, 2008). Mitochondrial DNA from BAR flies differs from WT mtDNA by 9 SNPs, mostly in protein-coding genes (Wolff et al., 2016a) (Fig. 1). All fly strains are kept in a strict breeding regime, whereby female flies from all strains are consistently backcrossed to the isogenic $w^{1118–5095}$ nuclear background, which itself is propagated via full-sub crosses. This regime ensures that all fly strains maintain the nuclear background as similar as possible.

For the purposes of the fitness experiment, competitor flies were used to mate with our focal (mitochondrial) flies. These competitor flies were from the outbred *D. melanogaster* genotype LH_M (Rice et al., 2005) and reared in the exact same conditions as experimental mitochondrial flies. Outbred flies were used to ensure that the focal flies were breeding with competitors of the highest possible fitness so all fertility responses were attributable to the focal flies alone.

4.2. NAC media preparation

For conditions requiring the antioxidant N-Acetyl-L-cysteine (NAC - Sigma A7250), fly food media was prepared at concentrations of 1 mg/mL and 10 mg/mL. For this, the desired quantity of NAC was dissolved in 100 mL of water and added to 900 mL of liquid fly food media. Once the NAC solution and liquid media were thoroughly mixed, 4 mL of NAC food were dispensed into individual fly vials. Powdered NAC and media stocks were stored at 4 °C and warmed to room temperature before use.

4.3. Fertility assay and survival to reproduction estimates

For these experiments males and females were assayed separately but following the same experimental rearing regime. Newly eclosed virgin *D. melanogaster* adults from the BAR, COXII or WT strains were immobilised through exposure to low concentrations of CO_2 (5 ppm), split by sex and transferred to vials containing treatment media at 0 (Control), 1 or 10 mg/mL NAC. Each vial contained three males or three females from one strain and each combination of media/strain had forty replicates per group (N = ~120 flies).

Flies were maintained on their respective treatment media for twelve days and transferred to new treatment media three times a week. After twelve days on treatment media, flies were transferred to vials containing standard control media and which had three competitor flies of the opposite sex to mate with. Flies were transferred to new media after two days and then adults discarded after a further two days. Eggs lain on media during each two-day period were allowed to develop at a constant 25 °C for fourteen days after which fertility was determined by a count of all adult progeny present in each vial.

Survival was measured as the percentage of each *D. melanogaster* strain for each media/sex combination that had survived by the final (16th) day of the fertility assay. Fly survival was recorded every time flies were swapped onto new food during the experiment.

4.4. Drosophila reproductive tissue size

For male reproductive tissue measurements, 12-day old males corresponding to each mtDNA genotype and NAC treatment were dissected (total of 40 males per experimental treatment). For each individual, reproductive organs were extracted and placed on a microscope slide containing one drop of room temperature PBS solution. A cover slip was placed on top of the sample and an image was acquired using a Leica DMLB microscope. Surface area of testes and accessory glands for each image was acquired using ImageJ software.

Female ovaries were extracted individual flies of each experimental treatment when flies were 12 days of age. Ovaries were placed on a microscope slide containing a drop of PBS, and number of ovarioles was counted under a light microscope.

4.5. Longevity

Newly eclosed *D. melanogaster* adults from the BAR, COXII or WT strains were collected within a 24 our period from each density-controlled vial. Vials for each haplotype were combined in a small holding cage with a petri dish of molasses-cornmeal-yeast food and left for 48 h to mate. Following this 48-h period, flies were immobilised through exposure to low concentrations of CO_2 (5 ppm), split by sex and transferred to vials containing treatment media at 0 (Control), 1 or 10 mg/mL NAC. Each vial contained ten males or ten females from one strain and each combination of media/strain had ten replicates per group (N = ~100 flies). Flies were transferred to fresh vials of their corresponding NAC treatment, and their survival scored three times a week.

4.6. High-resolution respirometry

High-Resolution Respirometry with Fluorometry (HHR-Fluo) was conducted with an Oroboros Oxygraph-2 K (O2K). Calibration for O_2 sensors and for H_2O_2 detection via Amplex Ultra Red according to manufacturer's protocol. Protocols can be found online at www.bioblast.at. Thoracic muscle was permeabilised in ice cold BIOPS (CaK_2EGTA 2.77 mM, K_2EGTA7.23 mM, $MgCl_2{\cdot}6H_20$ 6.56 mM, Imidazole 20 mM, Taurine 20 mM, Na_2Phosphocreatine 15 mM, Dithiothreitol 0.5 mM, K-MES 50 mM, Na_2ATP 5.77 mM) containing 81.25 μg/mL Saponin for 30 min, with a subsequent 10 min wash in ice cold MiR05 buffer. Testes and ovaries were homogenised in *Drosophila* Ringer's buffer. Oxygen flux recordings were conducted in MiR05 ((pH 7.1) EGTA 0.5 mM, $MgCl_2.6H_2O$ 3 mM, Lactobionic Acid 60 mM, Taurine 20 mM, KH_2PO_4 10 mM, HEPES 20 mM, D-Sucrose 110 mM, BSA (essentially fatty acid free) 1 g/L) with the additions of Pyruvate (10 mM), Malate (10 mM), and L-Proline (10 mM), as well as HRP (2 units) and Amplex Ultra Red (10 μM) prior to insertion of sample. Oxygen Flux rates were measured before and after additions of ADP (5 mM) to observe State 3 respiration, Succinate (10 mM) to reach State 3 for CI + CII, snGlycerol-3-phosphate (10 mM) to achieve state 3 for CI + CII + G3PDH, and FCCP was titrated (0.25 μM increments) until the sample reached maximum uncoupled State 3 (State 3u). Once State 3u was reached the sequential addition of the inhibitors Rotenone (0.5uM) and Antimycin A (2.5 uM) allowed the estimation of CI and CII+ G3PDH relative contributions to overall flux. O_2 and H_2O_2 flux rates were normalised to total protein (mg) in chamber by conducting Pierce™ BCA total protein quantification assay (Thermo Fisher Scientific) either directly from homogenate sample, or by homogenizing thoraces retrieved from the O2K recording chambers. For each experimental unit (mito/tissue/treatment/sex combination) we collected between 6 and 8 replicates.

4.7. Glutathione assay

Intracellular reduced and total glutathione levels were quantified using the bioluminescent Promega GSH-Glo™ glutathione assay (Promega), as recommended by the supplier. In brief, 5 thoraces, 40 ovaries and 60 testes were extracted from flies of each experimental treatment (in triplicate). Individual samples were first dissected and held in ice-cold Drosophila Ringers Buffer (1×) while dissections were underway. Samples were then spun down at 8000 ×*g* for 5 min at 4 °C. Supernatant was removed and replaced with 100 μL of DPBS+0.2 mM of

EDTA. Samples were then homogenised in this buffer, and later centrifuged at 1700 ×*g* for 10 min (4 °C). Supernatant was transferred to a new microtube and stored at −80 °C until time of assay.

For the assay, 15ul of each experimental sample were used to measure reduced glutathione and total glutathione separately on a 384-well plate (Greiner). For total glutathione measurements, 1 mM of TCEP was added to each well and incubated at RT for 30 min. To all samples, 15ul of 2× GSH-GloTM Reagent was added and samples were incubated for 30 min at RT. Following this incubation time, 30ul of Luciferin detection reagent was added to each well, mixed well using a shaker and incubated for 15 min. Luminescence was then measured using a Pherastar FS. A standard was run alongside all samples which included 5, 2.5, 1.25, 0.625, 0.3125,0.15625,0.078125 and 0 mg of glutathione. All samples were normalised to total protein concentration (mg) in the sample by using the Pierce™ BCA total protein quantification assay (Thermo Fisher Scientific).

4.8. Statistical analyses

Male and female phenotypic traits were analysed separately, as experiments were performed separately. For female fitness, the overall total number of offspring was zero-inflated. We therefore analysed this dataset using a negative binomial distribution (Mullahy, 1986), in which the zero values are a blend of sampling and structural effects (negative binomial parameter; variance = $\phi\mu$). These models were performed using the R (v. 3.0.2) package glmmADMB (http://glmmadmb.r-forge.r-project.org/glmmADMB.html). The response variable was total number of offspring produced, with mitochondrial haplotype and NAC treatment (plus their interaction) as fixed factors. Male offspring production was modelled by fitting a generalized linear mixed model, using a Gaussian distribution. For each analysis, mitochondrial strain and NAC treatment (plus their interaction) were modelled as fixed factors in the *lme4* package (Bates et al., 2012) in R (Fox, 2002).

Proportion survival to reproduction was modelled as a binomial vector, composed of total number of flies in the vial at the start of the experiment and number of flies that died, using a binomial distribution and logit link. Mitochondrial haplotype and NAC treatment (plus their interaction) were modelled as fixed factors. Analyses were performed using the *lme4* package (Bates et al., 2012) in R (Fox, 2002).

Reproductive morphological traits were analysed in two different ways. Male reproductive tissue surface area was modelled using a linear model, whereby area was a response variable, with mitochondrial genotype and NAC treatment (plus their interaction) as fixed effects. Female ovariole numbers were modelled using a general linear model with a quasipoisson distribution (to account for overdispersion of data). Ovariole number was the response variable, with mitochondrial genotype and NAC treatment (plus their interaction) as fixed effects. Models were implemented using the *lme4* package (Bates et al., 2012) in R (Fox, 2002).

Longevity analyses were performed using the *survival* package in R (Team, 2016; Therneau and Grambsch, 2000). We used Cox proportional hazard models, with survival as a response variable. Mitochondrial haplotype, NAC treatment and sex (plus all their interactions) were fixed effects in the model. We also investigated this dataset in a sex-specific manner. For this, we split the data into each sex respectively and ran models that included mtDNA and NAC treatment (plus their interactions) as fixed factors.

Metabolic continuous variables were centred and standardised prior analysis using the 'prcomp' function in R version 3.3.2 (Team, 2016). Most of the respiratory parameters were highly correlated to each other, therefore we used principal component analysis to reduce these variables to two linearly uncorrelated components. The two main principal components accounted for 96.78 % of the variance. Following the principal components analysis, we tested the significance of sex and tissue on PC1 and PC2. The main model had (residual) PC1 and PC2 as response variables, with tissue, sex and their interaction as fixed effects. We performed a Tukeys post-hoc test to determine which factors (sex and/or tissue) contributed to the overall multivariate effect. All analyses were performed using the *aov* and *TukeyHSD* functions in R version 3.3.2 (Team, 2016).

For subsequent metabolic analyses, we focused on key parameters that reflect mitochondrial respiration; State 3 oxygen, State 3 peroxide flux and glutathione. For these three traits we used linear models with either variable as response variables and sex, mitochondrial genotype and NAC as fixed factors (plus all their interactions). Further analyses included using Tukeys post-hoc test to identify which factors were contributing to the overall multivariate effect. Analyses were performed using the *lmer* and *TukeyHSD* functions in R version 3.3.2 (Team, 2016).

Funding

This work was supported by funding from the Biotechnology and Biological Sciences Research Council (BB/S003681/1) and bgc3 to NL and Leverhulme Trust (RPG-2019-109), UKRI Fellowship (NE/V014307/1) to MFC.

Data and materials availability

All data is accessible on Dryad repository.

CRediT authorship contribution statement

All authors contributed to the conception and writing of the paper. MFC carried out the phenotypic work. VK, HC & ER carried out the fluorespirometry. All authors analysed the results. MFC, ER and NL wrote the MS.

Declaration of competing interest

NL is a member of the SAB of Metro International Biotech.

Data availability

All data is accessible on Dryad repository

Acknowledgments

General: We thank Rebecca Finlay for help with running experiments.

Appendix A. Supplementary data

Supplementary data to this article can be found online at https://doi.org/10.1016/j.exger.2023.112158.

References

Ameur, A., Stewart, J.B., Freyer, C., Hagstrom, E., Ingman, M., Larsson, N.G., Gyllensten, U., 2011. Ultra-deep sequencing of mouse mitochondrial DNA: mutational patterns and their origins. PlosGenet. 7.

Aw, W.C., Garvin, M.R., Melvin, R.G., Ballard, J.W.O., 2017. Sex-specific influences of mtDNA mitotype and diet on mitochondrial functions and physiological traits in drosophila melanogaster. PLOS ONE 12, e0187554.

Baris, T.Z., Wagner, D.N., Dayan, D.I., Du, X., Blier, P.U., Pichaud, N., Oleksiak, M.F., Crawford, D.L., 2017. Evolved genetic and phenotypic differences due to mitochondrial-nuclear interactions. PLoS Genet. 13, e1006517.

Barja, G., 2013. Updating the mitochondrial free radical theory of aging: an integrated view, key aspects, and confounding concepts. Antioxid. Redox Signal. 19, 1420–1445.

Barreto, F.S., Watson, E.T., Lima, T.G., Willett, C.S., Edmands, S., Li, W., Burton, R.S., 2018. Genomic signatures of mitonuclear coevolution across populations of *Tigriopus californicus*. Nat. Ecol. Evol. 2, 1250–1257.

Bates, D., Maechler, M., Bolkler, B., 2012. lme4: Linear mixed-effects models using S4 classes. R package version 0999999-0. http://CRANR-projectorg/package=lme4.

Beer, S.M., Taylor, E.R., Brown, S.E., Dahm, C.C., Costa, N.J., Runswick, M.J., Murphy, M.P., 2004. Glutaredoxin 2 catalyzes the reversible oxidation and

glutathionylation of mitochondrial membrane thiol proteins: implications for mitochondrial redox regulation and antioxidant DEFENSE. J. Biol. Chem. 279, 47939–47951.
Bénit, P., El-Khoury, R., Schiff, M., Sainsard-Chanet, A., Rustin, P., 2010. Genetic background influences mitochondrial function: modeling mitochondrial disease for therapeutic development. Trends Mol. Med. 16, 210–217.
Bjelakovic, G., Nikolova, D., Gluud, C., 2014. Antioxidant supplements and mortality. Curr. Opin. Clin. Nutr. 17, 40–44.
Bjelakovic, G., Nikolova, D., Gluud, L.L., Simonetti, R.G., Gluud, C., 2007. Mortality in randomized trials of antioxidant supplements for primary and secondary prevention - systematic review and meta-analysis. J. Am. Med. Assoc. 297, 842–857.
Blagosklonny, M.V., 2013. Aging is not programmed: genetic pseudo-program is a shadow of developmental growth. Cell Cycle 12, 3736–3742.
Blier, P.U., Dufresne, F., Burton, R.S., 2001. Natural selection and the evolution of mtDNA-encoded peptides: evidence for intergenomic co-adaptation. Trends Genet. 17, 400–406.
Brack, C., Bechter-Thuring, E., Labuhn, M., 1997. N-acetylcysteine slows down ageing and increases the life span of Drosophila melanogaster. Cell. Mol. Life Sci. 53, 960–966.
Brand, M.D., 2016. Mitochondrial generation of superoxide and hydrogen peroxide as the source of mitochondrial redox signaling. Free Radic.Biol. Med. 100, 14–31.
Camus, M.F., Clancy, D.J., Dowling, D.K., 2012. Mitochondria, maternal inheritance, and male aging. Curr. Biol. 22, 1717–1721.
Camus, M.F., Dowling, D.K., 2018. Mitochondrial genetic effects on reproductive success: signatures of positive intrasexual, but negative intersexual pleiotropy. Proc. R.Soc. BBiol. Sci. 285.
Camus, M.F., O'Leary, M., Reuter, M., Lane, N., 2020. Impact of mitonuclear interactions on life-history responses to diet, 375.
Camus, M.F., Wolf, J.B., Morrow, E.H., Dowling, D.K., 2015. Single nucleotides in the mtDNA sequence modify mitochondrial molecular function and are associated with sex-specific effects on fertility and aging. Curr. Biol. 25, 2717–2722.
Clancy, D.J., 2008. Variation in mitochondrial genotype has substantial lifespan effects which may be modulated by nuclear background. Aging Cell 7, 795–804.
D'Aquila, P., Bellizzi, D., Passarino, G., 2015. Mitochondria in health, aging and diseases: the epigenetic perspective. Biogerontology 16, 569–585.
de Paula, W.B.M., Lucas, C.H., Agip, A.-N.A., Vizcay-Barrena, G., Allen, J.F., 2013. Energy, ageing, fidelity and sex: oocyte mitochondrial DNA as a protected genetic template. Philos. Trans. R. Soc. B Biol. Sci. 368, 20120263.
Eslamieh, M., Williford, A., Betran, E., 2017. Few nuclear-encoded mitochondrial gene duplicates contribute to male germline-specific functions in humans. Genome Biol. Evol. 9, 2782–2790.
Forte, M., Palmerio, S., Bianchi, F., Volpe, M., Rubattu, S., 2019. Mitochondrial complex I deficiency and cardiovascular diseases: current evidence and future directions. J. Mol. Med. 97, 579–591. Berl.
Fox, J., 2002. An R And S-Plus Companion to Applied Regression. Sage Publications, Thousand Oaks, Calif.
Gallach, M., Chandrasekaran, C., Betran, E., 2010. Analyses of nuclearly encoded mitochondrial genes suggest gene duplication as a mechanism for resolving intralocus sexually antagonistic conflict in Drosophila. Genome Biol. Evol. 2, 835–850.
Guarás, A., Perales-Clemente, E., Calvo, E., Acín-Pérez, R., Loureiro-Lopez, M., Pujol, C., Martínez-Carrascoso, I., Nuñez, E., García-Marqués, F., Rodríguez-Hernández, M.A., Cortés, A., Diaz, F., Pérez-Martos, A., Moraes, C.T., Fernández-Silva, P., Trifunovic, A., Navas, P., Vazquez, J., Enríquez, J.A., 2016. The CoQH2/CoQ ratio serves as a sensor of respiratory chain efficiency. Cell Rep. 15, 197–209.
Gui, D.Y., Sullivan, L.B., Luengo, A., Hosios, A.M., Bush, L.N., Gitego, N., Davidson, S.M., Freinkman, E., Thomas, C.J., Vander Heiden, M.G., 2016. Environment dictates dependence on mitochondrial complex I for NAD+ and aspartate production and determines cancer cell sensitivity to metformin. Cell Metab. 24, 716–727.
Halliwell, B., 2011. Free radicals and antioxidants - quo vadis? Trends Pharmacol. Sci. 32, 125–130.
Halliwell, B., 2013. The antioxidant paradox: less paradoxical now? Br. J. Clin. Pharmacol. 75, 637–644.
Hamanaka, R.B., Chandel, N.S., 2010. Mitochondrial reactive oxygen species regulate cellular signaling and dictate biological outcomes. Trends Biochem. Sci. 35, 505–513.
Havird, J.C., McConie, H.J., 2019. Sexually antagonistic mitonuclear coevolution in duplicate oxidative phosphorylation genes. Integr. Comp. Biol. 59, 864–874.
Healy, T.M., Burton, R.S., 2020. Strong selective effects of mitochondrial DNA on the nuclear genome. Proc. Natl. Acad. Sci. U. S. A. 117, 6616–6621.
Holper, L., Ben-Shachar, D., Mann, J.J., 2019. Multivariate meta-analyses of mitochondrial complex I and IV in major depressive disorder, bipolar disorder, schizophrenia, Alzheimer disease, and Parkinson disease. Neuropsychopharmacology 44, 837–849.
Inigo, M., Deja, S., Burgess, S.C., 2021. Ins and outs of the TCA cycle: the central role of anaplerosis. Annu. Rev. Nutr. 41, 19–47.
Innocenti, P., Morrow, E.H., Dowling, D.K., 2011. Experimental evidence supports a sex-specific selective sieve in mitochondrial genome evolution. Science 332, 845–848.
Ji, Z., Liu, G.H., Qu, J., 2022. Mitochondrial sirtuins, metabolism, and aging. J. Genet. Genomics 49, 287–298.
Kauppila, T.E.S., Kauppila, J.H.K., Larsson, N.G., 2017. Mammalian mitochondria and aging: an update. Cell Metab. 25, 57–71.
Khan, N.A., Nikkanen, J., Yatsuga, S., Jackson, C., Wang, L., Pradhan, S., Kivela, R., Pessia, A., Velagapudi, V., Suomalainen, A., 2017. mTORC1 regulates mitochondrial integrated stress response and mitochondrial myopathy progression. Cell Metab. 26, 419–428 e415.
Kopinski, P.K., Janssen, K.A., Schaefer, P.M., Trefely, S., Perry, C.E., Potluri, P., Tintos-Hernandez, J.A., Singh, L.N., Karch, K.R., Campbell, S.L., Doan, M.T., Jiang, H., Nissim, I., Nakamaru-Ogiso, E., Wellen, K.E., Snyder, N.W., Garcia, B.A., Wallace, D. C., 2019. Regulation of nuclear epigenome by mitochondrial DNA heteroplasmy. Proc. Natl. Acad. Sci. U. S. A. 116, 16028–16035.
Korge, P., Calmettes, G., Weiss, J.N., 2015. Increased reactive oxygen species production during reductive stress: the roles of mitochondrial glutathione and thioredoxin reductases. Biochim. Biophys. Acta 1847, 514–525.
Lagouge, M., Larsson, N.G., 2013. The role of mitochondrial DNA mutations and free radicals in disease and ageing. J. Intern. Med. 273, 529–543.
Lane, N., 2011. Mitonuclear match: optimizing fitness and fertility over generations drives ageing within generations. BioEssays 33, 860–869.
Lane, N., 2012. The problem with mixing mitochondria. Cell 151, 246–248.
Lane, N., 2022. Transformer: The Deep Chemistry of Life And Death. WW Norton.
Larsson, N.G., 2010. Somatic mitochondrial DNA mutations in mammalian aging. Annu. Rev. Biochem. 79, 683–706.
Latorre-Pellicer, A., Moreno-Loshuertos, R., Lechuga-Vieco, A.V., Sanchez-Cabo, F., Torroja, C., Acin-Perez, R., Calvo, E., Aix, E., Gonzalez-Guerra, A., Logan, A., Bernad-Miana, M.L., Romanos, E., Cruz, R., Cogliati, S., Sobrino, B., Carracedo, A., Perez-Martos, A., Fernandez-Silva, P., Ruiz-Cabello, J., Murphy, M.P., Flores, I., Vazquez, J., Enriquez, J.A., 2016. Mitochondrial and nuclear DNA matching shapes metabolism and healthy ageing. Nature 535, 561–565.
Lee, K.P., Simpson, S.J., Clissold, F.J., Brooks, R., Ballard, J.W.O., Taylor, P.W., Soran, N., Raubenheimer, D., 2008. Lifespan and reproduction in Drosophila: New insights from nutritional geometry. Proc. Natl. Acad. Sci. U. S. A. 105, 2498–2503.
Lord, T., Nixon, B., 2020. Metabolic changes accompanying spermatogonial stem cell differentiation. Dev. Cell 52, 399–411.
Mailloux, R.J., 2020. Protein S-glutathionylation reactions as a global inhibitor of cell metabolism for the desensitization of hydrogen peroxide signals. Redox Biol. 32, 101472.
Mailloux, R.J., Willmore, W.G., 2014. S-glutathionylation reactions in mitochondrial function and disease. Front. Cell Dev. Biol. 2, 68.
Mallay, S., Gill, R., Young, A., Mailloux, R.J., 2019. Sex-dependent differences in the bioenergetics of liver and muscle mitochondria from mice containing a deletion for glutaredoxin-2. Antioxidants 8. Basel.
Manolio, T.A., Collins, F.S., Cox, N.J., Goldstein, D.B., Hindorff, L.A., Hunter, D.J., McCarthy, M.I., Ramos, E.M., Cardon, L.R., Chakravarti, A., Cho, J.H., Guttmacher, A.E., Kong, A., Kruglyak, L., Mardis, E., Rotimi, C.N., Slatkin, M., Valle, D., Whittemore, A.S., Boehnke, M., Clark, A.G., Eichler, E.E., Gibson, G., Haines, J.L., Mackay, T.F., McCarroll, S.A., Visscher, P.M., 2009. Finding the missing heritability of complex diseases. Nature 461, 747–753.
Martinez-Reyes, I., Chandel, N.S., 2020. Mitochondrial TCA cycle metabolites control physiology and disease. Nat. Commun. 11, 102.
McDonald, A.E., Pichaud, N., Darveau, C.A., 2018. "Alternative" fuels contributing to mitochondrial electron transport: importance of non-classical pathways in the diversity of animal metabolism. Comp. Biochem. Physiol. B Biochem. Mol. Biol. 224, 185–194.
McFarland, R., Clark, K.M., Morris, A.A.M., Taylor, R.W., Macphail, S., Lightowlers, R.N., Turnbull, D.M., 2002. Multiple neonatal deaths due to a homoplasmic mitochondrial DNA mutation. Nat. Genet. 30, 145–146.
Montooth, K.L., Dhawanjewar, A.S., Meiklejohn, C.D., 2019. Temperature-sensitive reproduction and the physiological and evolutionary potential for mother's curse. Integr. Comp. Biol. 59, 890–899.
Morgan, B., Van Laer, K., Owusu, T.N., Ezerina, D., Pastor-Flores, D., Amponsah, P.S., Tursch, A., Dick, T.P., 2016. Real-time monitoring of basal H2O2 levels with peroxiredoxin-based probes. Nat. Chem. Biol. 12, 437–443.
Morrow, E.H., Camus, M.F., 2017. Mitonuclear epistasis and mitochondrial disease. Mitochondrion 35, 119–122.
Morrow, E.H., Reinhardt, K., Wolff, J.N., Dowling, D.K., 2015. Risks inherent to mitochondrial replacement. EMBO Rep. 16, 541–544.
Mossman, J.A., Tross, J.G., Jourjine, N.A., Li, N., Wu, Z., Rand, D.M., 2017. Mitonuclear interactions mediate transcriptional responses to hypoxia in Drosophila. Mol. Biol. Evol. 34, 447–466.
Mossman, J.A., Tross, J.G., Li, N., Wu, Z., Rand, D.M., 2016. Mitochondrial-nuclear interactions mediate sex-specific transcriptional profiles in Drosophila. Genetics 204, 613–630.
Mota-Martorell, N., Jove, M., Pradas, I., Sanchez, I., Gomez, J., Naudi, A., Barja, G., Pamplona, R., 2020. Low abundance of NDUFV2 and NDUFS4 subunits of the hydrophilic complex I domain and VDAC1 predicts mammalian longevity. Redox Biol. 34, 101539.
Mullahy, J., 1986. Specification and testing of some modified count data models. J. Econ. 33, 341–365.
Murphy, M.P., 2009. How mitochondria produce reactive oxygen species. Biochem. J. 417, 1–13.
Nacarelli, T., Azar, A., Sell, C., 2015. Aberrant mTOR activation in senescence and aging: a mitochondrial stress response? Exp. Gerontol. 68, 66–70.
Neiman, M., Taylor, D.R., 2009. The causes of mutation accumulation in mitochondrial genomes. Proc. Biol. Sci. 276, 1201–1209.
Niraula, P., Kim, M.S., 2019. N-acetylcysteine extends lifespan of drosophila via modulating ROS scavenger gene expression. Biogerontology 20, 533–543.
Pamplona, R., Jové, M., Mota-Martorell, N., Barja, G., 2021. Is the NDUFV2 subunit of the hydrophilic complex I domain a key determinant of animal longevity? FEBS J. 288, 6652–6673.
Patel, M.R., Miriyala, G.K., Littleton, A.J., Yang, H., Trinh, K., Young, J.M., Kennedy, S. R., Yamashita, Y.M., Pallanck, L.J., Malik, H.S., 2016. A mitochondrial DNA

hypomorph of cytochrome oxidase specifically impairs male fertility in Drosophila melanogaster. elife 5.
Pesole, G., Allen, J.F., Lane, N., Martin, W., Rand, D.M., Schatz, G., Saccone, C., 2012. The neglected genome. EMBO Rep. 13, 473–474.
Picard, M., Shirihai, O.S., 2022. Mitochondrial signal transduction. Cell Metab. 34, 1620–1653.
Quinlan, C.L., Perevoshchikova, I.V., Hey-Mogensen, M., Orr, A.L., Brand, M.D., 2013. Sites of reactive oxygen species generation by mitochondria oxidizing different substrates. Redox Biol. 1, 304–312.
Quiros, P.M., Mottis, A., Auwerx, J., 2016. Mitonuclear communication in homeostasis and stress. Nat. Rev. Mol. Cell Biol. 17, 213–226.
Rand, D.M., Clark, A.G., Kann, L.M., 2001. Sexually antagonistic cytonuclear fitness interactions in Drosophila melanogaster. Genetics 159, 173–187.
Rank, N.E., Mardulyn, P., Heidl, S.J., Roberts, K.T., Zavala, N.A., Smiley, J.T., Dahlhoff, E.P., 2020. Mitonuclear mismatch alters performance and reproductive success in naturally introgressed populations of a montane leaf beetle. Evolution. 74, 1724–1740.
Rice, W.R., Linder, J.E., Friberg, U., Lew, T.A., Morrow, E.H., Stewart, A.D., 2005. Inter-locus antagonistic coevolution as an engine of speciation: Assessment with hemiclonal analysis. Proc. Natl. Acad. Sci. U. S. A. 102, 6527–6534.
Rodenburg, R.J., 2016. Mitochondrial complex I-linked disease. Biochim. Biophys. Acta 1857, 938–945.
Rodriguez-Nuevo, A., Torres-Sanchez, A., Duran, J.M., De Guirior, C., Martinez-Zamora, M.A., Boke, E., 2022. Oocytes maintain ROS-free mitochondrial metabolism by suppressing complex I. Nature 607, 756–761.
Salminen, A., Kauppinen, A., Hiltunen, M., Kaarniranta, K., 2014. Krebs cycle intermediates regulate DNA and histone methylation: epigenetic impact on the aging process. Ageing Res. Rev. 16, 45–65.
Samuni, Y., Goldstein, S., Dean, O.M., Berk, M., 2013. The chemistry and biological activities of N-acetylcysteine. Biochim. Biophys. Acta 1830, 4117–4129.
Shaposhnikov, M.V., Zemskaya, N.V., Koval, L.A., Schegoleva, E.V., Zhavoronkov, A., Moskalev, A.A., 2018. Effects of N-acetyl-L-cysteine on lifespan, locomotor activity and stress-resistance of 3 Drosophila species with different lifespans. Aging (Albany NY) 10, 2428–2458.
Sobotta, M.C., Liou, W., Stocker, S., Talwar, D., Oehler, M., Ruppert, T., Scharf, A.N., Dick, T.P., 2015. Peroxiredoxin-2 and STAT3 form a redox relay for H2O2 signaling. Nat. Chem. Biol. 11, 64–70.
Song, S., Pursell, Z.F., Copeland, W.C., Longley, M.J., Kunkel, T.A., Mathews, C.K., 2005. DNA precursor asymmetries in mammalian tissue mitochondria and possible contribution to mutagenesis through reduced replication fidelity. Proc. Natl. Acad. Sci. U. S. A. 102, 4990–4995.
Sweetlove, L.J., Beard, K.F., Nunes-Nesi, A., Fernie, A.R., Ratcliffe, R.G., 2010. Not just a circle: flux modes in the plant TCA cycle. Trends Plant Sci. 15, 462–470.
Team, R.C., 2016. R: A Language And Environment for Statistical Computing.
Therneau, T.M., Grambsch, P.M., 2000. Modeling Survival Data: Extending the Cox Model. Springer, New York.
Trifunovic, A., Hansson, A., Wredenberg, A., Rovio, A.T., Dufour, E., Khvorostov, I., Spelbrink, J.N., Wibom, R., Jacobs, H.T., Larsson, N.G., 2005. Somatic mtDNA mutations cause aging phenotypes without affecting reactive oxygen species production. Proc. Natl. Acad. Sci. U. S. A. 102, 17993–17998.
Trivers, R., Campbell, B., 1972. Parental investment and sexual selection. In: Sexual Selection And the Descent of Man 1871-1971. Aldine-Atherton, Chicago (IL).
Vander Heiden, M.G., Cantley, L.C., Thompson, C.B., 2009. Understanding the Warburg effect: the metabolic requirements of cell proliferation. Science 324, 1029–1033.
Vasan, K., Werner, M., Chandel, N.S., 2020. Mitochondrial metabolism as a target for cancer therapy. Cell Metab. 32, 341–352.
Wallace, D.C., Fan, W., 2010. Energetics, epigenetics, mitochondrial genetics. Mitochondrion 10, 12–31.
Wei, Y.H., Zhang, Y.J., Cai, Y., Xu, M.H., 2015. The role of mitochondria in mTOR-regulated longevity. Biol. Rev. 90, 167–181.
Weinberg, F., Chandel, N.S., 2009. Mitochondrial metabolism and cancer. Ann. N. Y. Acad. Sci. 1177, 66–73.
Wetzker, C., Reinhardt, K., 2019. Distinct metabolic profiles in Drosophila sperm and somatic tissues revealed by two-photon NAD(P)H and FAD autofluorescence lifetime imaging. Sci. Rep. 9, 19534.
Willems, P.H.G.M., Rossignol, R., Dieteren, C.E.J., Murphy, M.P., Koopman, W.J.H., 2015. Redox homeostasis and mitochondrial dynamics. Cell Metab. 22, 207–218.
Wolff, J.N., Camus, M.F., Clancy, D.J., Dowling, D.K., 2016a. Complete mitochondrial genome sequences of thirteen globally sourced strains of fruit fly (Drosophila melanogaster) form a powerful model for mitochondrial research. Mitochond. DNA A 27, 4672–4674.
Wolff, J.N., Ladoukakis, E.D., Enriquez, J.A., Dowling, D.K., 2014. Mitonuclear interactions: evolutionary consequences over multiple biological scales. Philos. Trans. R. Soc. Lond. Ser. B Biol. Sci. 369, 20130443.
Wolff, J.N., Pichaud, N., Camus, M.F., Cote, G., Blier, P.U., Dowling, D.K., 2016b. Evolutionary implications of mitochondrial genetic variation: mitochondrial genetic effects on OXPHOS respiration and mitochondrial quantity change with age and sex in fruit flies. J. Evol. Biol. 29, 736–747.
Xiao, W., Loscalzo, J., 2020. Metabolic responses to reductive stress. Antioxid. Redox Signal. 32, 1330–1347.
Zaidi, A.A., Makova, K.D., 2019. Investigating mitonuclear interactions in human admixed populations. Nat. Ecol. Evol. 3, 213–222.
Zhang, H., Limphong, P., Pieper, J., Liu, Q., Rodesch, C.K., Christians, E., Benjamin, I.J., 2012. Glutathione-dependent reductive stress triggers mitochondrial oxidation and cytotoxicity. FASEB J. 26, 1442–1451.
Zhong, L., Mostoslavsky, R., 2011. Fine tuning our cellular factories: sirtuins in mitochondrial biology. Cell Metab. 13, 621–626.
Zhu, C.-T., Ingelmo, P., Rand, D.M., 2014. G×G×E for lifespan in Drosophila: mitochondrial, nuclear, and dietary interactions that modify longevity. PLoS Genet. 10, e1004354.